J. Fluid Mech. (1998), *vol.* 377, *pp.* 137–149. Printed in the United Kingdom

Observation of cusps during the levelling of free surfaces in viscous flows

By S. BETELÚ, R. GRATTON AND J. DIEZ†

Instituto de Física Arroyo Seco, Facultad de Ciencias Exactas, Universidad Nacional del Centro de la Provincia de Buenos Aires, Pinto 399, 7000, Tandil, Argentina

(Received 22 September 1997 and in revised form 23 July 1998)

We experimentally study the formation of cusps at the free surfaces of viscous fluids in three simple cases that portray possible natural or industrial procceses. Two cases concern levelling driven by gravity: the case (A) of a sinusoidal surface and the case (B) of a single groove. In the third case (C), an initially sinusoidal surface evolves under the action of a fast enough lateral compression that the effects of gravity are negligible. Case (A) shows a critical aspect ratio above which the cusps form. Case (B) allows a more detailed study of the evolution of the cuspidal structure, which does not change in shape but reduces its size according to a simple power law dependence in time. In case (C), cusps form even for small initial aspect ratios.

1. Introduction

The levelling of a rippled free surface of a very viscous liquid may occur in non-trivial ways, which merit attention both for theoretical and practical reasons. Let us consider, for instance, a smoothly perturbed horizontal free surface: even in the simplest case in which gravity is the only driving force, the levelling process may pass through a stage characterized by the presence of sharp grooves with cuspidal entrances. This problem was numerically studied by Pozrikidis (1997) for a sinusoidal perturbation. He found that only below a critical aspect ratio (amplitude to wavelength ratio) of the initial corrugation do the ripples damp out more or less exponentially with time, but that above this critical value, cuspidal entrances appear at the bottom of the valleys while the summits remain smooth. Once the cuspidal entrances form, they become smaller and smaller as the levelling proceeds, but as far as those results show, the vertex lines remain sharply defined and can be regarded as singular lines of the surface, where the direction of the outgoing normal changes abruptly by 180°.

Cuspidal entrances like those appearing in the above quoted numerical simulations seem to be typical surface structures of Stokes flows. They originate in a variety of situations, and have received considerable attention in the last years. For instance, Joseph *et al.* (1991) and Jeong & Moffatt (1992) experimentally studied steady cusps formed at the surface of a viscous liquid in a basin with the flow driven by rotating cylinders. Jeong & Moffatt also found an exact solution of the Stokes equation that describes a steady flow near a cusp. When capillary forces are present, the 'cusp' has strictly speaking a rounded apex, but the maximum curvature is an exponentially increasing function of the capillary number, and becomes extremely large even for relatively low values of this number. In a different line of work,

† Author to whom correspondence should be addressed (email: jdiez@exa.unicen.edu.ar).

Howison & Richardson (1995) found solutions that describe the formation of cusps on the surface of cylindrical drops sucked from their axis, and Tanveer & Vasconcelos (1994, 1995) studied their appearance at the surface of rippled cylindrical bubbles immersed in a convergent flow. Also, Liu, Liao & Joseph (1995) investigated the cusp that forms at the lower part of an ascending bubble. Recently (Marino, Thomas & Gratton 1997), it was noted that the entrance below the prominent nose of a creeping current in the neighbourhood of the contact line presents the essential characteristics of a cuspidal entrance.

A noteworthy property of these structures is that the apex line moves at a finite speed with respect to the fluid, in such a way that the free surface elements are convected inside the fluid bulk through the cusp, whose apex line could be regarded as a 'sink' of the free surface. Accordingly, cusps are expected to form when and where the flow enforces a strong decrease of the free surface area. A similar situation may arise in quite natural ways, such as the above mentioned levelling of a rippled surface by gravity, the lateral squeezing of the fluid between rigid walls, etc. The formation of cusps is, then, a process of practical interest which not only affects the surface morphology but also provides a mechanism for conveying surface material into the bulk of a viscous fluid.

Here we describe experiments concerning the formation and evolution of cusps at the surface of a very viscous fluid in the three simple cases sketched in figure 1. Case (A) corresponds to the above mentioned numerical study by Pozrikidis, i.e. the levelling due to gravity of a free surface initially perturbed by a sinusoidal ripple. In agreement with Pozrikidis' results, if the initial aspect ratio of the perturbation is high enough, its shape changes strongly during the levelling. Even though the peak to peak amplitude always decreases, cusps form in the valleys. In case (B) the flow is also driven by gravity alone, but the initial perturbation is a deep single groove of approximately triangular shape. A large cusp forms very soon at the bottom of the groove, so that its evolution may be followed with accuracy. The profile of the surface resembles that of the steady cusp considered by Jeong & Moffatt (1992), though in our case the flow is unsteady. The size of the structure decreases gradually in a self-similar way till it becomes of the order of the capillary distance (≈ 0.13 cm for the fluid used). The last stage is a progressive smoothing of the profile attributable to capillarity. Finally, in case (C), the surface is initially perturbed as in case (A), but the flow is driven by a fast enough lateral compression so as to make gravity effects negligible. In spite of the apparent differences, we observe that the surface evolution associated with this flow retains many features of the surface evolution of a rippled cylindrical drop sucked from its axis, theoretically studied by Howison & Richardson (1995). Basically, cusps form at the bottom of the valleys and a decrease in size of the entire cusped periodic structure follows without appreciable changes in the shape.

2. Experimental setup

We produce the flows within an uncovered rectangular box made of thick (1 cm) aluminium plates. Two opposite walls separated by 10 cm are fixed. The other two walls can slide driven by two independent screws, so that the distance between them may be gradually changed between 15 cm and 5 cm, thus allowing the squeezing of the fluid required in case (C) (figure 1). For cases (A) and (B), we keep this distance fixed to 11 cm.

The fluid is a silicon putty (Gomme GSIR, produced by Rhône-Poulenc) with viscosity $\nu \approx 1.5 \times 10^5$ S, $\rho = 1.12$ g cm^{-3} and surface tension $\gamma \approx 20$ dyn cm^{-1}. The

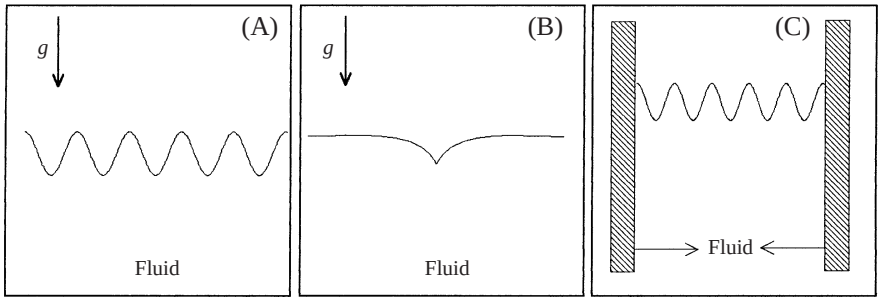

FIGURE 1. (A) Levelling of a rippled free surface driven by gravity alone, (B) levelling of a single groove and (C) squeezing of a corrugated free surface.

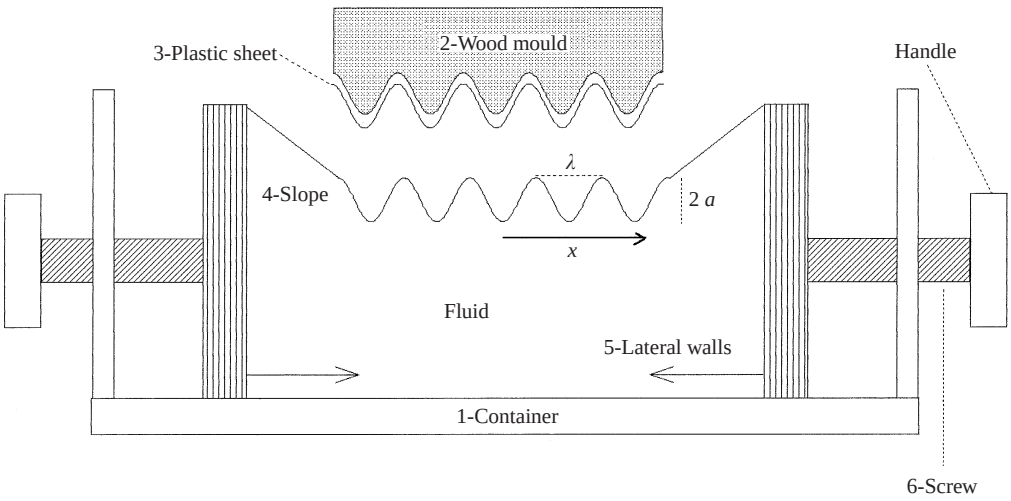

FIGURE 2. Experimental setup: the fluid (silicon putty) is in the container (1), the corrugated free surface is impressed with a mould (2), which is covered with a thin polythene sheet (3); the slopes (4) are present only in case (C).

perturbations of the free surface are impressed by means of wood moulds, covered with thin polythene sheets in order to avoid adherence between the wood and the fluid (see figure 2), so expediting removal. The ripples are always impressed parallel to the sliding walls. The experiments typically last between 10^2 to 10^3 s and involve scale lengths of a few centimetres. It is well known that a viscous fluid of that high viscosity is not usually Newtonian, but it was observed that in this range of strain rates, the putty does not depart very much from a Newtonian behaviour (see the Appendix). Therefore, the observed evolutions of the free surfaces are reasonable representations of what should be expected for Stokes flows.

We observe the height profiles $h(x, t)$ with the aid of a simple optical system. A plane sheet of light is generated by expanding and collimating a He-Ne laser beam with a combination of cylindrical and convergent lenses. This sheet illuminates the free surface of the opaque putty, generating there a bright line about 0.02 cm thick, which is recorded with a CCD camera. We choose the orientation of both the plane of incidence of the light sheet and of the axis of the camera in such a way that the luminous line portrays the profile $h(x, t)$ of the free surface without appreciable distortions.

In the interpretation of the results we always assume that the fluid velocity in the transversal y-direction (i.e. along the grooves) is negligible and, in general, that the dependence on this coordinate may be neglected within the observation region. This assumption is reasonable near the middle vertical plane of the box, separated from the fixed walls by distances considerably larger than the scale of the surface perturbations under study. On the other hand, by means of naked eye observations of the free surface from the top, we take care that neither the direction nor the depth of the grooves change appreciably along y within the observation region.

3. Case (A): levelling of a periodic free surface

In this case the initial profile of the fluid is approximately given by $h(x,0) = h_0 + a_0 \sin 2\pi x/\lambda$. We use three moulds with the same value of $\lambda = 1.5$ cm, and different amplitudes, namely, $a_0 = 0.23$, 0.5 and 0.75 cm. We also change h_0 from 2 cm to about 5 cm; however, as this change does not produce significant effects we report here only the results corresponding to $h_0 = 4.5$ cm.

In figure 3 we show sequences of the profiles for $a_0 = 0.23$ cm and 0.75 cm. In the former case, whose aspect ratio is $a_0/\lambda = 0.153$, the free surface maintains its sinusoidal shape with an amplitude decreasing almost exponentially with time. This is in agreement with the theoretical solution valid for small amplitudes (Jeong & Moffat 1992) and infinite depth (linear approximation)

$$h(x,t) = a_0 \exp\left(-\frac{1}{4\pi}\frac{\lambda g t}{\nu}\right) \sin\left(2\pi\frac{x}{\lambda}\right). \tag{3.1}$$

In figure 4, we report the experimental time evolution of the amplitude in comparison with the exponential coefficient $a_0 \exp\left(-\lambda g t/4\pi\nu\right)$.

For the intermediate case ($a_0 = 0.5$ cm and $a_0/\lambda = 0.33$, not reported in the figures) the decrease of the amplitude is accompanied by a deformation of the profile: the valleys sharpen and the summits remain smooth; however, we do not observe cusps. For $a_0 = 0.75$ cm and $a_0/\lambda = 0.5$, the deformation becomes stronger as shown in figure 3(b). Figure 5, which is a magnified view of the evolution of a particular valley, shows the presence of a cusp at an intermediate stage ($t = 571$ s). For comparison, we plot the theoretical profile $y \propto x^{2/3}$ of a cusp (Joseph 1992; Joseph *et al.* 1991). The results suggest that there is a critical value of a_0/λ for which cusps appear, and that this value is between 0.33 and 0.5. This is fairly consistent with the numerical work of Pozrikidis (1997) (figure 8 of his work, where $a/H = 2a_0/\lambda$), where the critical aspect ratio a_0/λ is between 0.2 and 0.4. Though the threshold condition for cusp formation is not accurately obtained, the experiments show that cusps actually appear beyond some value of a_0/λ.

Note that the cusps are temporary; they tend to disappear under the effect of capillarity when the amplitude is of the order of the capillary length $a = (\gamma/\rho g)^{1/2} \approx 0.13$ cm. By using (3.1), the capillary number $Ca = \mu(\mathrm{d}h/\mathrm{d}t)/\gamma$ is given by $Ca = a_0\lambda/a^2$; thus, $Ca \approx 20$ in figure (3a) and $Ca \approx 66$ in figure (3b).

4. Case (B): levelling of a single perturbation

In order to study in more detail the evolution of a cusp during the levelling driven by gravity, we observe the evolution of a single large perturbation. We impress on the fluid an approximately triangular deep groove of 4 cm width and 7 cm depth in the middle of the container. Initially, the apex of the groove is close to the bottom of the

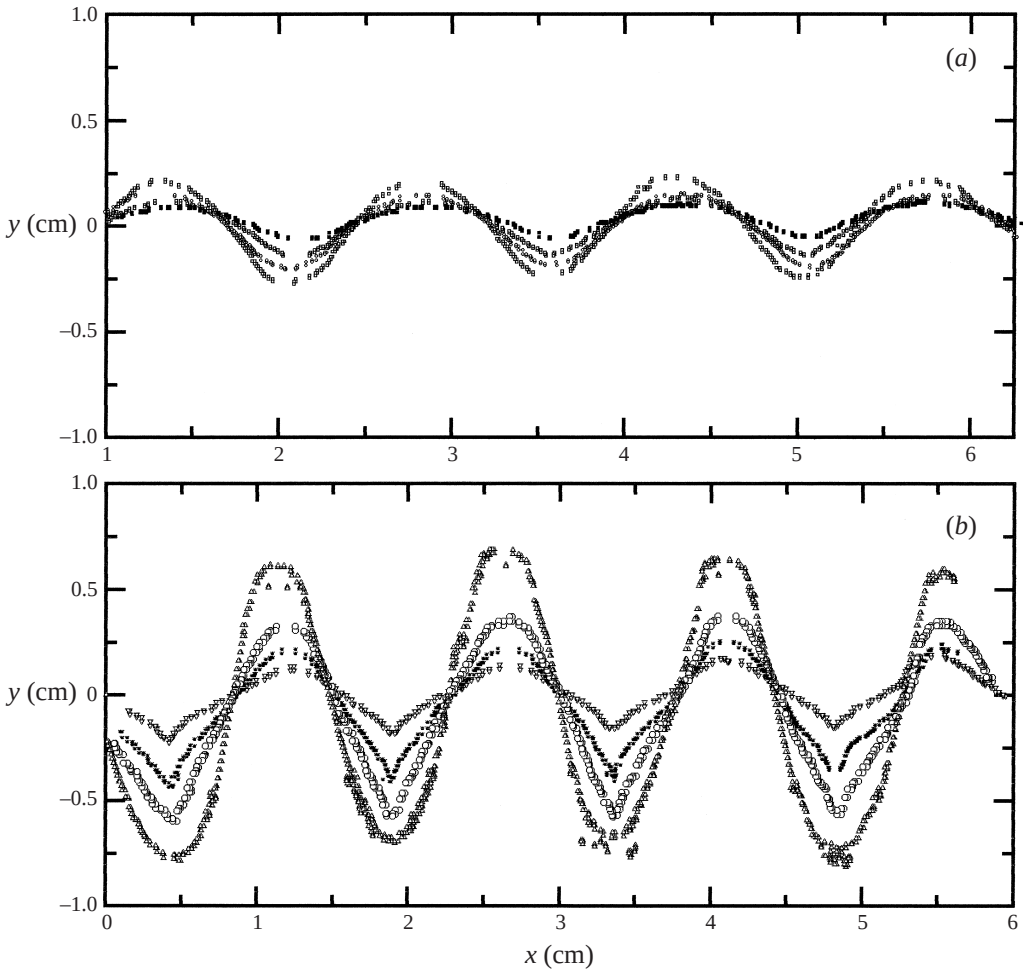

FIGURE 3. Viscous–gravity levelling (case A) for: (*a*) $a_0 = 0.23$ cm and $\lambda = 1.5$ cm; the profiles correspond to the times $t = 3$, 302, 604 and 1178 s. (*b*) $a_0 = 0.75$ cm and $\lambda = 1.5$ cm; the profiles correspond to the times $t = 30$, 305, 604 and 1205 s.

container. Soon afterwards, a cusp appears at the rapidly lifting apex. In figure 6(*a*) we show a relatively advanced stage of the evolution of the free surface, where a cusp in the bottom of the groove is clearly seen. Successive profiles have different size but approximately the same shape. By scaling all the lengths with the depth $\delta(t)$ (distance between the apex of the cusp and the maximum height), we find that all the profiles have the same shape, as shown in figure 6(*b*). This means that this stage of the evolution is self-similar; we verify that this is true almost independently of the details of the initial groove shape. In the neighbourhood of the apex, the height profile may be approximated by $y/\delta \simeq 0.85(x/\delta)^{2/3}$ (see figure 6*b*).

Figure 7 shows the time evolution of the depth $\delta(t)$, which is well fitted by the power law $\delta(t) = 2.1\nu/gt$. This dependence may be explained in terms of a simple balance of forces, namely the gravity buoyancy force, that is the weight of the liquid that would fill the groove, $F_g \sim \rho g \delta^2 L$ (where $L = 1$ is the unit length along the groove) and the viscous force (stress due to a typical gradient of velocity $\mu(\mathrm{d}\delta/\mathrm{d}t)/\delta$ times the area where this stress acts, of magnitude $\sim L\delta$) $F_\mu \sim -\mu((\mathrm{d}\delta/\mathrm{d}t)/\delta)L\delta$. It

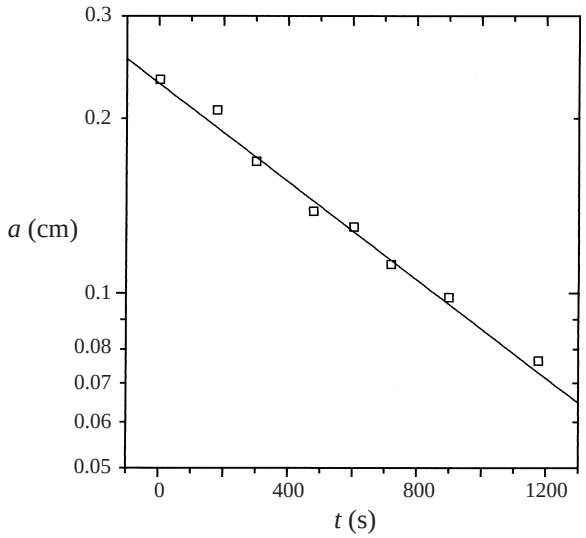

FIGURE 4. Amplitude vs. time for the levelling of a sinusoidal corrugation (case A) with $a_0 = 0.23$ cm.

follows that

$$\rho g \delta^2 \sim -\mu \frac{\mathrm{d}\delta}{\mathrm{d}t}, \tag{4.1}$$

and integrating, we obtain the scaling law

$$\delta(t) \sim \frac{\mu}{\rho g t}, \tag{4.2}$$

whose coefficient is approximately 2.1 according to our experiments.

In principle, in a flow without capillarity, the cusp should remain indefinitely. But in a real fluid it becomes rounded when the capillary number $Ca = \mu(\mathrm{d}\delta/\mathrm{d}t)/\gamma$ becomes of the order of unity; therefore, the cusp disappears when δ becomes of the order of the capillary length a. In this experiment, Ca varies from 21 at the beginning of the experiment to 0.95 at the end, when the cusp starts to disappear.

5. Case (C): compression of a free surface

In the compression experiments, the initial surface profile is the same as in case (A), but the decrease of the surface area is now due to the compression of the fluid in the x-direction between the two moving walls of the box. However, since the surface of a slab of fluid squeezed in this way suffers strong long-scale deformations, some special cautions must be adopted. In fact, the surface tends to rise in the middle and to curl near the moving walls, mainly because the fluid cannot slip at the walls. A simple way to overcome this difficulty is sketched in figure 2: the corrugated region under study is connected to the moving walls by two fluid regions 2.5 cm wide with an about uniform slope. We empirically found that when a fluid so modelled is squeezed between two walls moving at equal speed, the central region of the free surface lifts almost uniformly; besides, the approaching grooves remain approximately equidistant, thus showing that the compression is also practically uniform.

The second point is that, in contrast to case (A), we intend to produce a surface evolution little affected by both gravity and capillarity. Therefore, the compression

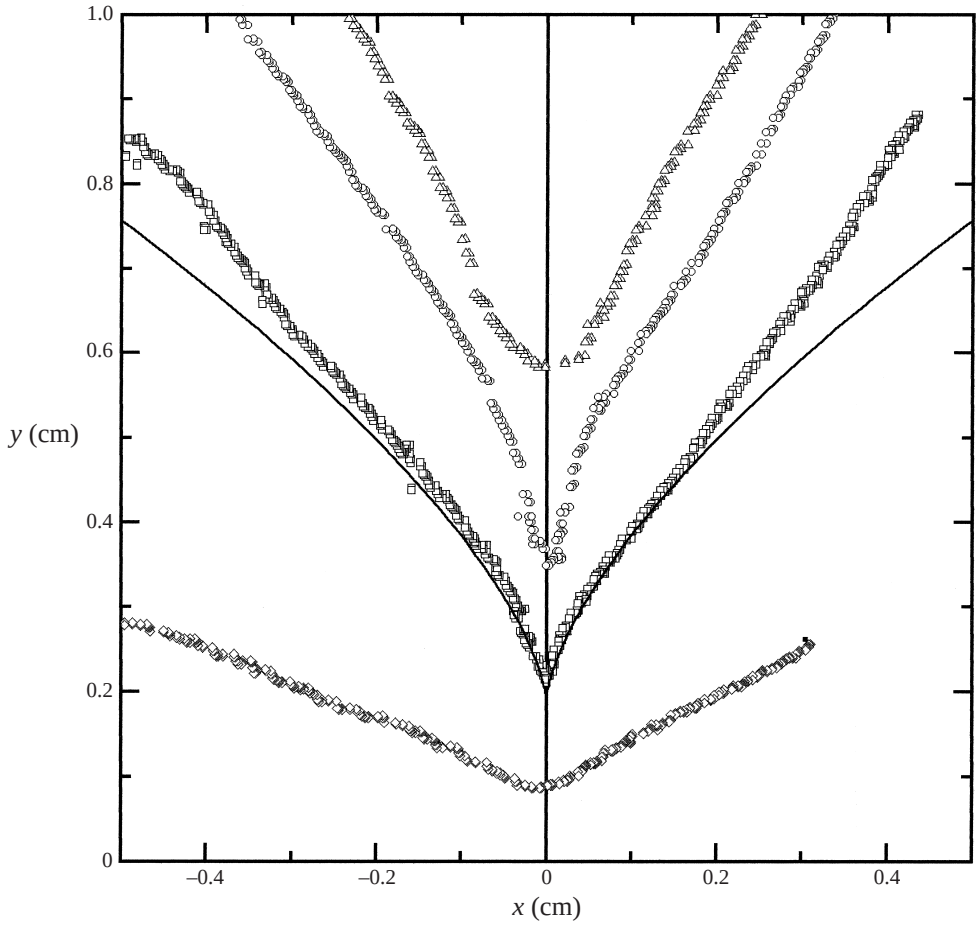

FIGURE 5. Magnified representation of a valley in an experiment with the same initial condition as figure 3(*b*) (case A), for times 251, 378, 571 and 1686 s. The line is the power law $y \propto x^{2/3}$.

should be completed in a time short in comparison with the decay time of a small-amplitude perturbation due to gravity alone. As this time is about 10^3 s (see case (A)), we design the experiments in order to obtain a compression ratio $\lambda_0/\lambda_{end} \approx 2$ in about 110 s. The speed v of each lateral wall is, then, of the order of 0.02 cm s^{-1}, and the corresponding capillary number $Ca = v\mu/\gamma$ is about 120, thus ensuring that capillary effects are negligible.

In figure 8 we show the evolution of the free surface for $\lambda_0 = 1.5$ cm and $a_0 = 0.12$ cm; it is clearly seen that cusps appear in the valleys. Since the corresponding aspect ratio is $a_0/\lambda = 0.08$, well below the limit found in case (A), their formation must be ascribed to the compression.

The sequence of figure 8 is representative of the behaviour observed for other aspect ratios, and differs very much from case (A). There is a first stage, before the formation of the cusps, characterized by an increase of the aspect ratio of the ripple; the wavelength shortens while the amplitude grows. This is the behaviour expected *prima facie* in a pure straining flow, where every parcel shrinks horizontally and expands vertically by the same factor. However, the growth of the aspect ratio is accompanied by a visible sharpening of the valleys which finally results in the

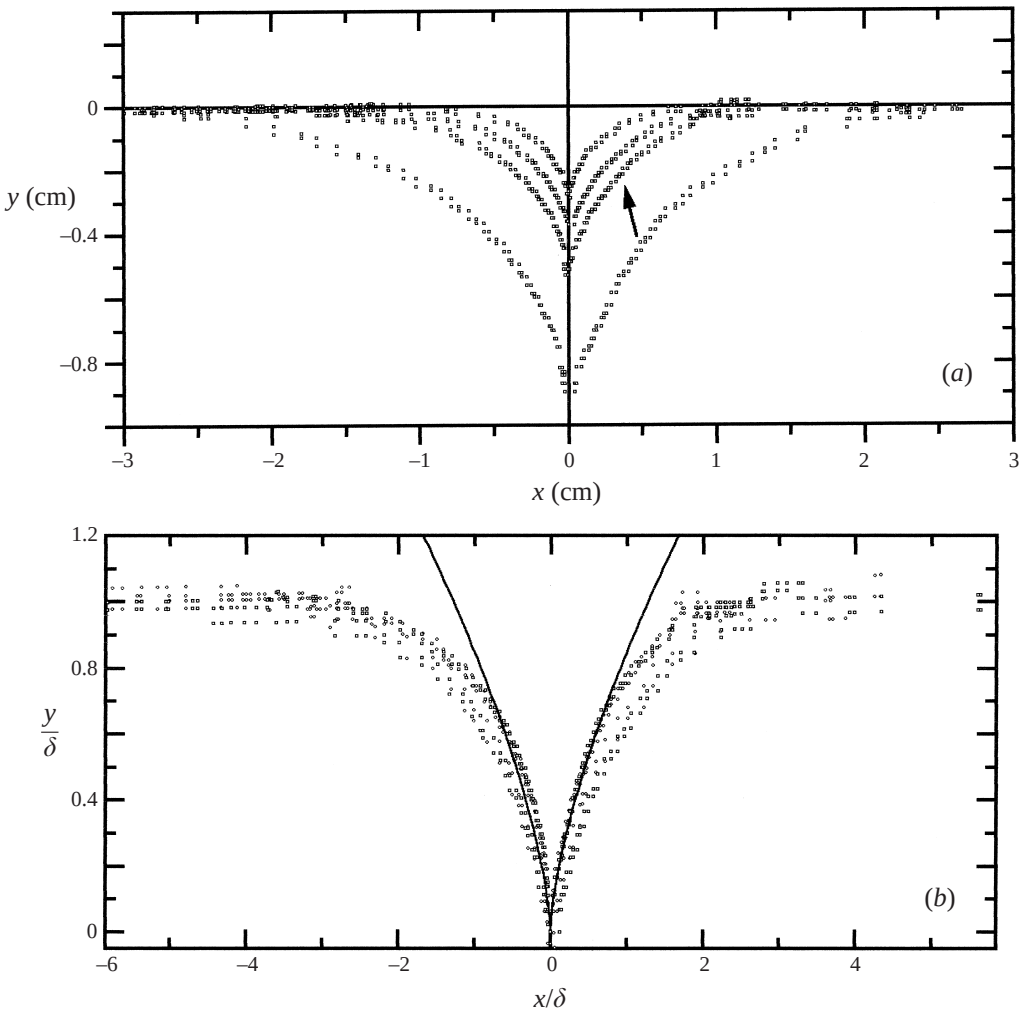

FIGURE 6. (*a*) Sequence of the height profiles for a single groove (case B), $t = 275.6$, 497.6, 672.4 and 967.9 s; the time evolution is indicated by the arrow. (*b*) Same profiles scaled with the depth $\delta(t)$.

formation of cusps. During the following second stage, the wavelength of the ripple continues to decrease according to the compression, but the amplitude decreases too, in such a way that the shape of the perturbation remains about invariant.

6. Discussion and conclusions

The results obtained in case (A) show a very good quantitative agreement with the theory for the linear damping of a small-amplitude ripple. For large amplitudes, the experiments qualitatively agree with the numerical simulations of Pozrikidis, and the critical aspect ratio a_0/λ for the cusp appearance is consistent with his results. Also, the size of the cusped entrance of case (B) decays as predicted by a simple and general dimensional model. These elements, together with the rheological behaviour reported in the Appendix, provide confidence that the observed behaviours are representative of those expected for a Newtonian fluid, i.e. that the effects related to the rheology

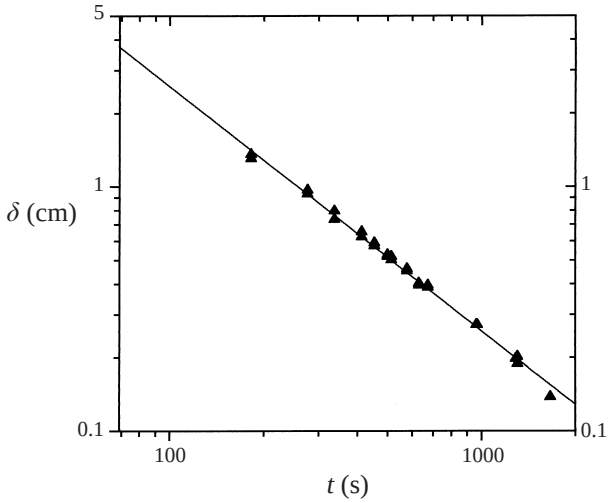

FIGURE 7. Depth $\delta(t)$ vs. time for a single groove (case B). The solid line is the law $\delta(t) = 2.1\nu/gt$.

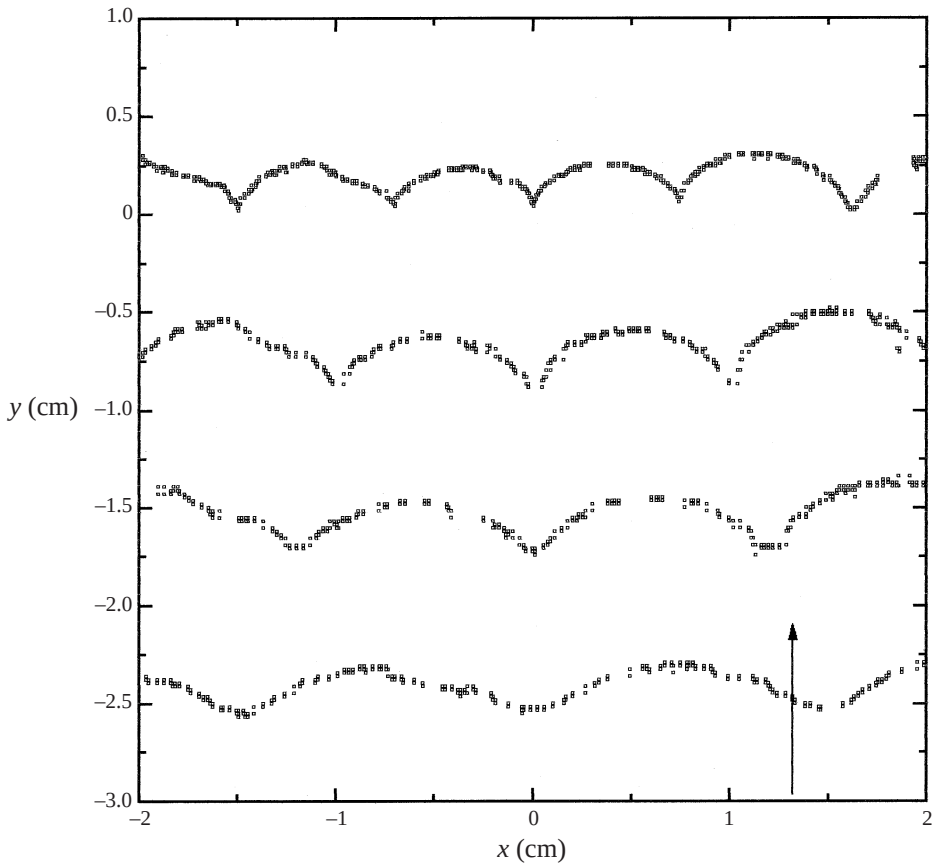

FIGURE 8. Sequence of height profiles for a squeezed fluid (case C); the initial corrugation has $a_0 = 0.12$ cm and $\lambda_0 = 1.5$ cm. The times are: $t = 14$, 43.5, 63 and 126 s, and the corresponding wavelengths are $\lambda = 1.5$, 1.2, 1.0, and 0.75 cm.

of the particular putty used are not substantial in the range of the shear rates of the experiments.

In all the cases, capillarity does not prevent the formation of near cusps provided that the corresponding capillary number Ca is larger than unity in the neighbourhood of the apex. If the flow is driven only by gravity, as in cases (A) and (B), this condition means that the capillary distance should be smaller than the typical length scale of the perturbation. Therefore, the effect of the capillarity in gravity-driven flows is to smooth the cusps when they become small, thus limiting the presence of the cusps to an intermediate stage of the ripple evolution. This apparently does not happen in case (C), since the capillary number is related to the speed of advance of the lateral walls, and it is very large as long as the walls move, so that the smoothing of the cusps due to the capillarity is not relevant.

It is interesting to consider the results of case (C) having in mind the exact solution of Howison & Richardson (1995) for a cylindrical drop with an arbitrary number of ripples at the surface that is being sucked by a linear sink in the centre. When the number of ripples is very large, we can focus on a small region near the free surface, which looks like a corrugated plane. As the drop is sucked, the surface shrinks, thus producing a compression of the ripples similar to those originated by the lateral compressing of case (C). Basically, cusps form at the bottom of the valleys and a decrease in size of the entire cusped periodic structure follows without appreciable changes in the shape. The similarity with our experiment is marked. Naturally, the shapes of the surface in both problems are not the same, but they share two features, namely that the surface shrinks in both cases and that the characteristic profile is of the form $y \propto x^{2/3}$ in the neighbourhood of the cusp (see, for instance, figure 6*b* for case (B)).

Finally, we want to point out that the process studied may actually occur in flows of viscous melted plastics, asphalts, lava, muds, etc. The condition is that viscous forces must dominate over capillary forces, i.e. the capillary number should be large compared with unity. It is likely that the rheology of the fluid is not a critical point. In order to verify this fact, we repeated the compression experiment (C) using pottery clay (strongly non-Newtonian). The observed evolution of the free surface, including the formation of cusps, resembles very closely that of the experiments with silicon putty.

This work was supported by the Consejo Nacional de Investigaciones Científicas y Técnicas (CONICET, Argentina), the Comisión de Investigaciones Científicas de la Provincia de Buenos Aires (CICPBA, Argentina), and the Universidad Nacional del Centro de la Provincia de Buenos Aires (Argentina). We wish to thank Dr Luis P. Thomas and Dr Beatriz Marino for their participation in the measurements reported in the Appendix.

Appendix

In view of the high viscosity of the silicon putty (Rhöne-Poulenc) used in our experiments, its rheological behaviour merits special attention. This behaviour was investigated by using a rotational viscometer specially built in the laboratory for this purpose. The device is a wide-gap concentric cylinder viscometer which allows one to measure the torque τ required for a spindle to rotate an angle θ inside the putty. The spindle of radius R_s (≈ 0.5 cm) hangs from a wire of length $l = 31.3$ cm and is immersed to a depth $L = 9.2$ cm into a large volume of silicon putty prepared as for

the experiments. After an initial angular displacement ($\simeq 0.1$ rad), the spindle returns to equilibrium with a decreasing angular velocity $\omega = -\mathrm{d}\theta/\mathrm{d}t$. A light beam deviated by a small mirror placed at the top of the spindle allows one to measure the angular deviation $\theta(t)$ on a far screen (the motion of the luminous point is recorded with a video camera).

As is usual we shall assume that the relation between the shear stress σ and the strain rate ε is given by a power-law relationship (Ostwald fluid)

$$\sigma = k\,|\varepsilon|^n, \tag{A 1}$$

where $0 < n < 1$ for shear-thinning fluids. In particular, σ and ε at the wall of the spindle are given by (Barnes, Hutton & Walters 1989)

$$\sigma = \frac{\tau}{2\pi R_s^2 L}, \tag{A 2}$$

$$\varepsilon = \frac{2\omega}{n\left(1 - b^{2/n}\right)}, \tag{A 3}$$

where b is the ratio of the spindle radius R_s to the external cylinder radius $R_c = 5$ cm ($b = 0.1$). On the other hand, the torsional rigidity $C = \tau/\theta$ of a cylindrical rod (wire) is given by (Landau & Lifshitz 1986):

$$C = \frac{G\pi r^4}{2l}, \tag{A 4}$$

where G ($\approx 9.16 \times 10^{11}$ g cm^{-2}) is the modulus of rigidity of the material (steel) and r its radius. Upon substitution into (A 1) we get

$$\sigma = \frac{G}{4R_s^2 l L}\theta r^4 = \kappa\omega^n, \tag{A 5}$$

where

$$\kappa = \left[2/n\left(1 - b^{2/n}\right)\right]^n. \tag{A 6}$$

In figure 9 we plot σ as a function of ω for three different ratios of the wire in order to cover a long interval of stresses. To convert the abscissa into values of ε it is necessary to determine n as a function of ω. Currently, this is done by dividing the domain into several intervals small enough to assure a constant value of n in each one. For our purpose, we simply observe that $n = 1$ (Newtonian behaviour) is a good approximation for $\omega > 2 \times 10^{-4}$, while $n \approx 0.6$ describes well the behaviour for $\omega < 5 \times 10^{-5}$. Consistently, our silicon putty behaves like a Newtonian fluid for $\varepsilon = \varepsilon_c > 4 \times 10^{-4}$ s^{-1} with a viscosity $\mu \approx 1.5 \times 10^5$ P, and like an Ostwald fluid for $\varepsilon < 1.67 \times 10^{-4}$ s^{-1}. Note that our measurements show that if there is a yield stress σ_0, it should be less than 2 dyn cm^{-2}. Besides, no viscoelastic behaviour was observed in the explored range of strain rates.

In case (A), the strain rate may be estimated as $h_t/h \approx \lambda g/v \approx 10^{-3}$ s^{-1} (see (3.1)). Analogously, in case (B) it is given by $\delta_t/\delta \approx t^{-1} > 10^{-3}$ s^{-1} (see (4.2)). Finally, ε for the case (C) is of the order of $v/h_0 \approx 4 \times 10^{-3}$ s^{-1}, since $v = 0.02$ cm s^{-1} and $h_0 \approx 4.5$ cm. As regards to the stresses, we see that typical values are given by the hydrostatic pressure $\rho g a \approx 10^3$ dyn cm^{-2}, which is much greater than any possible yield stress and corresponds to the Newtonian region of the rheological curve. Since all these typical values of ε are greater than ε_c, we see that the cusping experiments are all well inside the region of Newtonian behaviour of our silicon putty. This is in agreement with the observed exponential decay of a small-amplitude sinusoidal

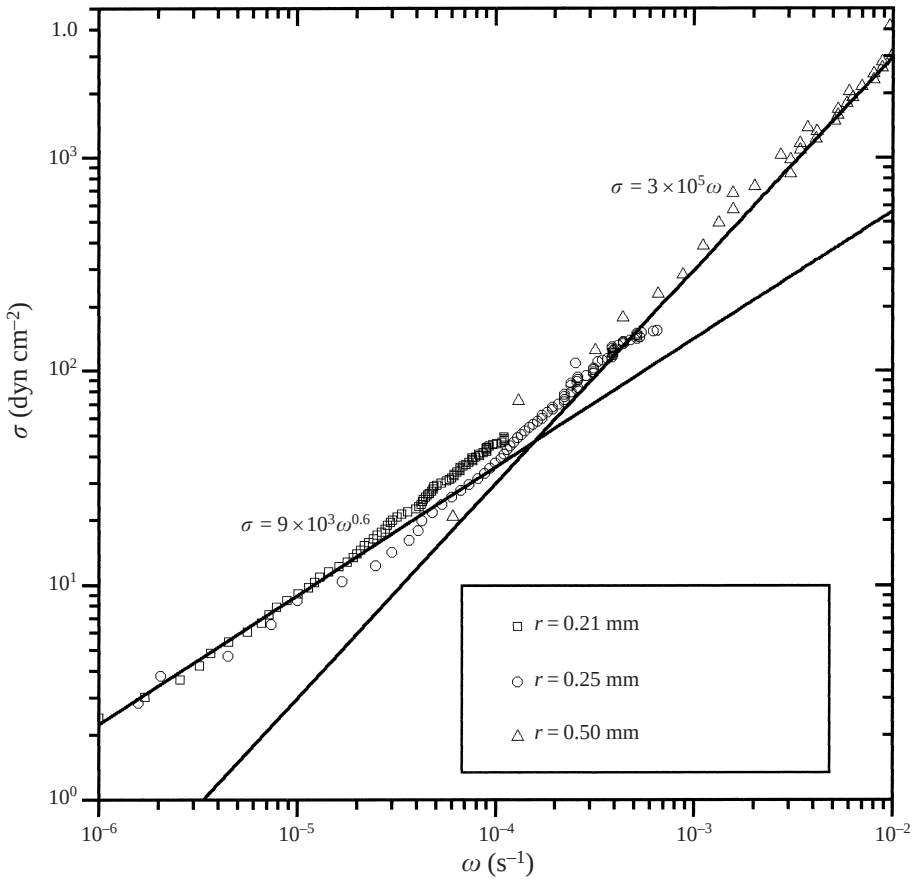

FIGURE 9. Rheological measurements of the silicon putty.

corrugation (see figures 3*a* and 4). In fact, a rheology-dependent effect might be observed in this case since the regions of larger slope (and thus larger stress) evolve according to a local viscosity smaller than that in regions of zero slope. However, this effect is so small that it escapes from observation.

It should be mentioned that the results for our silicon putty (figure 9) are quite different from those reported in Dixon & Sumers (1986) for another silicon putty, namely Dow Corning Dilatant Compound 3179. In that paper, the authors found $\varepsilon_c = 10^0$ s^{-1}, $n = 1/7$ and a yield stress $\sigma_0 \approx 3250$ dyn cm^{-2}. As a consequence, their silicon putty would not have been an appropriate material to perform our experiments.

REFERENCES

BARNES, H. A., HUTTON, J. F. & WALTERS, K. 1989 *An Introduction to Rheology*. Elsevier.

DIXON, J. M. & SUMMERS, J. M. 1986 Another word on the rheology of silicone putty: Bingham. *J. Structural Geol.* **8**, 593–595.

HOWISON, S. D. & RICHARDSON, S. 1995 Cusp development in free boundaries, and two-dimensional slow viscous flow. *Eur. J. Appl. Maths* **6**, 441–454.

JEONG, J. & MOFFATT, H. K. 1992 Free-surface cusps associated with flow at low Reynolds number. *J. Fluid Mech.* **241**, 1–22.

JOSEPH, D. D. 1992 Understanding cusped interfaces. *J. Non Newtonian Fluid Mech.* **44**, 127–148.

JOSEPH, D. D., NELSON, J., RENARDY, M. & RENARDY, Y. 1991 Two-dimensional cusped interfaces. *J. Fluid Mech.* **223**, 383–409.

LANDAU, L. D. & LIFSHITZ, E. M. 1986 *Theory of Elasticity*, 3rd Edn. Pergamon.

LIU, Y. J., LIAO, T. Y. & JOSEPH, D. D. 1995 A two-dimensional cusp at the trailing edge of an air bubble rising in a viscoelastic liquid. *J. Fluid Mech.* **304**, 321–342.

MARINO, B. M., THOMAS, L. P. & GRATTON, R. 1997 Shape and size of a current head in creeping flows. *Phys. Rev.* E **55**, 4296–4301.

POZRIKIDIS, C. 1997 Numerical studies of singularity formation at free surfaces and fluid interfaces in two-dimensional Stokes flow. *J. Fluid Mech.* **331**, 145–167.

TANVEER, S. & VASCONCELOS, G. L. 1994 Bubble breakup in two-dimensional Stokes flow. *Phys. Rev. Lett*. **73**, 2845–2848.

TANVEER, S. & VASCONCELOS, G. L. 1995 Time evolving bubbles in two-dimensional Stokes flow. *J. Fluid Mech.* **301**, 325–344.